**Pollen-Pistil Interactions in Tristylous Pontederia sagittata (Pontederiaceae). I. Floral Heteromorphism and Structural Features of the Pollen Tube Pathway**

Robin W. Scribailo; Spencer C. H. Barrett

*American Journal of Botany*, Vol. 78, No. 12 (Dec., 1991), 1643-1661.

Stable URL:
http://links.jstor.org/sici?sici=0002-9122%28199112%2978%3A12%3C1643%3APIITPS%3E2.0.CO%3B2-T

*American Journal of Botany* is currently published by Botanical Society of America.

American Journal of Botany 78(12): 1643–1661. 1991.

# POLLEN-PISTIL INTERACTIONS IN TRISTYLOUS PONTEDERIA SAGITTATA (PONTEDERIACEAE). I. FLORAL HETEROMORPHISM AND STRUCTURAL FEATURES OF THE POLLEN TUBE PATHWAY[1]

ROBIN W. SCRIBAILO[2] AND SPENCER C. H. BARRETT

Department of Botany, University of Toronto, Toronto, Ontario, Canada M5S 3B2

Heteromorphic characters and structural features of the pollen tube pathway are described in tristylous *Pontederia sagittata* to assess their influence on the pollination process and in mediating self-incompatibility behavior. Heteromorphic characters that distinguish the floral morphs include style length, stigma depth, stigmatic papillae length, stylar parenchyma cell length, area of the stylar canal, stamen height, anther size, and pollen size. Unlike several distylous species that have been investigated, the exine of pollen in *P. sagittata* was not strongly differentiated among the pollen types, and no differences in stigma cytochemistry were apparent. Features common to the floral morphs were a wet stigma, a hollow trilobed stylar canal separating into two sterile and one fertile canal, and a single anatropous ovule with a highly elaborated integumentary obturator. The similarity in structural features of the pollen tube pathway of *P. sagittata* to those found in monocotyledonous taxa with gametophytic self-incompatibility suggests that phylogenetic constraints may have influenced the evolution of trimorphic incompatibility in the Pontederiaceae.

Several hypotheses have been proposed to explain the functional significance of the floral polymorphisms that are found in heterostylous plants (Ganders, 1979; Barrett, 1990). Darwin (1877) suggested that the reciprocal stamen and style lengths that occur in the floral morphs evolved to facilitate insect-mediated cross-pollination among morphs with anthers and stigmas at equivalent heights. Similarly, Lloyd and Webb (In press a, b) have argued that the morphological features of heterostyly have been selected to improve the proficiency of cross-pollination. It has also been suggested that heteromorphic characters may play a direct role in the physiological functioning of the incompatibility system in heterostylous plants (Mather and DeWinton, 1941; Lewis 1942, 1943). Dulberger (1975a, b) has argued that differential growth of reproductive organs may be involved in the synthesis of incompatibility specificities and that heteromorphic features of pollen and stigmas aid in promoting the adhesion, hydration, and germination of compatible pollen grains. In virtually all heterostylous plants in which incompatibility has been demonstrated it is associated with heteromorphic characters of pollen and stigmas (Dulberger, 1975a; Ganders, 1979). Structural and physiological studies of several distylous taxa have suggested that certain ancillary heteromorphic characters associated with the stamen-style polymorphism may influence various aspects of incompatibility behavior (Dulberger, 1974, 1981, 1987, 1989; Ghosh and Shivanna, 1980a, b, 1982; Shivanna, Heslop-Harrison, and Heslop-Harrison, 1981, 1983; Stevens and Murray, 1982; Schou, 1984; Schou and Mattsson, 1985).

The potential role of heteromorphic characters in influencing pollen-pistil interactions in tristylous taxa has not been considered in any detail. Flowers of tristylous species exhibit two distinct pollen types produced by the contrasting stamen levels within a flower. The pollen types differ in both size and incompatibility phenotype, a feature unique among angiosperms (Esser, 1953; Ornduff, 1966; Dulberger, 1970; Barrett, 1977). It is not known to what extent trimorphic incompatibility results

[1] Received for publication 22 October 1990; revision accepted 25 July 1991.

The authors thank Fanny Strumas and William Cole for technical assistance; Brian Husband, Charles Fenster, and Michele Dudash for advice; Steve Scribailo for assistance with Fig. 3; and Nancy Dengler, Rivka Dulberger, Michele Heath and Steven Seavey for comments on an earlier draft of the manuscript. This paper represents part of a doctoral dissertation presented to the Department of Botany, University of Toronto by RWS. The work was supported by an NSERC postgraduate scholarship and University of Toronto open fellowships to RWS and an NSERC operating grant to SCHB.

[2] Author for correspondence, current address: Biological Sciences and Chemistry Section, Purdue University, North Central Campus, Westville, IN 46391.

from biochemical differences in pollen that may be attributable to differences in sporophytic gene expression and/or physical interactions between the heteromorphic characters of pollen and pistil. A lack of information on the general properties of trimorphic incompatibility largely results from the limited number of investigations of pollen tube growth in tristylous plants (Esser, 1953; Dulberger, 1970; Anderson and Barrett, 1986). The overall purpose of the present study was to investigate the nature of pollen-pistil interactions in a tristylous plant, *Pontederia sagittata* Presl. (Pontederiaceae), by examining features of the pollen tube pathway and the structure and function of heteromorphic characters. In so doing we hoped to clarify how incompatibility operates in tristylous plants and how it might have originated within the Pontederiaceae.

In this paper we describe heteromorphic characters that distinguish the floral morphs of *P. sagittata* and structural features of the pollen tube pathway that are likely to influence incompatibility behavior. The specific questions addressed in our study were: What quantitative differences in mature floral organization distinguish the floral morphs? Do the floral morphs exhibit physical and cytochemical differences in pistil structure, with particular reference to stigma characteristics? What structural features of the pollen tube pathway are likely to influence patterns of pollen tube growth? In a companion paper (Scribailo and Barrett, 1991), quantitative aspects of pollen tube growth following compatible and incompatible pollinations are discussed in the context of the structural information presented in this study.

## MATERIALS AND METHODS

***Plant material***—Plants used in this study represent genetic stocks maintained since their collection from a population at Vera Cruz along the lowland coastal plain of Mexico in 1982 (see Glover and Barrett, 1983). Information on the reproductive ecology of populations, as well as quantitative data on pollen size and production and seed set following controlled legitimate and illegitimate pollinations are available in this publication. Clones of each genotype were grown as emergent aquatics, rooted in submersed plastic pots on a flooded bench, under glasshouse conditions. For all sampling of floral material, flowers were collected from different clones during the same time period (usually on the same day) and inflorescence positions to minimize environmental and developmental variation.

***Floral measurements***—To document floral features that characterize the tristylous syndrome, measurements were made on three clones per morph and ten flowers per clone. Measurements were made using a Zeiss SV-8 stereomicroscope equipped with a drawing tube. To facilitate measurements, a digitizing tablet was employed (Jandel Scientific Model 2200/2210 39C2) with SigmaScan software.

A series of traits was measured on each flower. The three stamens within each of the two stamen sets were measured for floral tube length below stamen insertion (distance between base of ovary and base of free filament of the stamen), free filament length, anther length, and anther width. For the pistil, ovary length, style length (including stigma), and stigma depth were measured. Stigma depth was measured as the distance between the base and tip of the stigma. The length of five stigmatic papillae was recorded for the stigmas of five pistils, 20 pistils per genotype, and three clones per morph using whole fixed pistils, cleared and stained for callose (see Scribailo and Barrett, 1991). Stained pistils were viewed under epifluorescence on a Zeiss Axioplan Universal microscope. The length of 20 stylar parenchyma cells was also measured for ten styles per genotype and three genotypes per morph using the same technique. Cell measurements were taken from the middle of the style from a single file of cells.

Comparisons of cross-sectional areas of the style and stylar canals of the morphs were made using the following method. Fresh styles were placed on a dental wax sheet under a dissecting microscope and cross sectioned, using a microdissection blade, into 2-mm pieces representing the top, middle, and base of each style. Style segments were then placed into 2-mm-deep and 0.8-mm-diameter wells machined into a plexiglass slide. A narrow, raised edge around the perimeter of the slide allowed it to be flooded with aniline blue stain (0.1% in 0.1 M triphosphate buffer) such that a 24 × 50-mm coverslip could be placed over but not touching the sections. The slide was viewed under epifluorescence with blue light (excitation 450–494 nm, dichroic mirror 510 nm, barrier 520 nm) on a Reichert Polyvar microscope equipped with a drawing tube. Fluorescence of cell walls allowed visualization of all features of the sections (see Fig. 37). Tracings were made of the perimeter of the style and of each stylar canal for each section. Sections from the top, middle, and base of the style were traced for each of ten styles for each clone. The cross-sectional areas of the style and stylar canals were then measured from the tracings using the digitizing tablet.

***Data analysis***—Data for all floral measurements were tested for homogeneity of variances using the $F_{max}$-test (Sokal and Rohlf, 1981). Variables with heterogeneous variances were either log- or square root-transformed. After ANOVA, means were compared with Scheffe's procedure at the 0.05 level (SAS version 6, 1987). For variables with heterogeneous variances after transformation, a Kruskal-Wallis test was performed (SAS version 6, 1987). Mean ranks were then compared using Dunn's multiple comparisons procedure at the 0.05 level (Hollander and Wolfe, 1973).

***Anatomy***—The following method was used to embed tissue for studies of the structural features of the pollen tube pathway. Pistils of the three morphs were removed from flowers with forceps and cut into pieces corresponding to the stigma, style, and ovary. Styles were then cut into additional 5-mm segments. Tissue was fixed for 6 hr in 2% glutaraldehyde in phosphate buffer (pH 6.8). Tissue was vacuum infiltrated shortly after placement in fixative to ensure good preservation. Samples were then washed four times 5 min in 0.05 M phosphate buffer with sucrose, postfixed 2 hr in 1% osmium tetroxide, washed three times for 5 min in phosphate buffer, and transferred through a graded ethanol series into absolute ethanol. Tissue was infiltrated through a propylene oxide series, passed through several changes of Epon plastic, and embedded (Luft, 1961). Thick (3-$\mu$m) transverse and longitudinal sections were made with glass knives using a Sorvall MT-2B ultramicrotome. Sections were stained with 0.1% toluidine blue in 0.1% sodium carbonate (pH 10.1).

***Scanning electron microscopy***—Fresh pollen was placed on stubs and viewed directly under the scanning electron microscope (SEM) without coating. Pistils were removed from the flowers with forceps and cut into segments corresponding to the stigma, style, and ovary. Tissue was then fixed for 6 hr in glutaraldehyde after initial vacuum infiltration, and washed four times for 5 min in phosphate buffer. At this point some stylar and ovarian tissue was further dissected in buffer under a dissecting microscope to expose features of the stylar canal and ovule. Samples were then transferred through a graded ethanol series into absolute ethanol. Tissue was critical-point dried in a custom-built "bomb" using carbon dioxide as the intermediate fluid, mounted on metal stubs, and coated with gold-palladium for 5 min in a Hummer VI sputter-coater. Specimens were viewed on a Hitachi Model S570 SEM at 10 kV.

***Cytochemistry***—To investigate the possibility of morph-specific differences in the cytochemistry of stigmas, a range of tests was conducted. All cytochemical tests were performed on fresh stigmas, stained and whole mounted in 30% glycerin. When not stated otherwise, stains were dissolved in distilled water, and their strengths refer to weight to volume of solvent. All staining was for 30 min. Most stigmas that were observed under white light were also viewed under fluorescence. Additional information on stain specificities can often be obtained in this manner since two sites with similar autofluorescence can show differential quenching after staining. The filter combination used for fluorescence microscopy was an ultraviolet (UV) system (Zeiss No. 2, exciter G-365, dichromatic beam splitter FT-395, barrier LP-420).

Lipids were stained with either saturated solutions of Sudan black B and Sudan III in 70% ethanol or Nile blue sulfate prepared as a 1% aqueous (water) solution (Jensen, 1962). In a fluorescent test for lipids, stigmas were treated with aqueous phosphine (chrysaniline yellow CI 46045) and viewed with UV light (Popper, 1944). Cutin and surface lipids were stained with 0.01% auramine O and also viewed under UV light (Heslop-Harrison and Shivanna, 1977).

The presence of proteins was detected using 0.025% Coomassie brilliant blue in a mixture of water, methanol, and acetic acid (v/v 87:10:3) (Heslop-Harrison, 1979) and by viewing under UV light after staining with 0.001% 1 anilinonaphthalene-8-sulfonic acid (1-ANS) (Fulcher and Wong, 1980). Carbohydrate determination was made using toluidine blue metachromacy (TBO) (Feder and O'Brien, 1968). A positive reaction with 1% alcian blue in 3% acetic acid was regarded as an indication of pectic substances and carboxylated polysaccharides (Jensen, 1962; Benes, 1968). Starch was localized using iodine potassium iodide (IKI) (Jensen, 1962). Nonspecific esterase activity was detected using naphthyl acetate as a substrate and fast blue BB salt as a coupler (Pearse, 1972). Controls were always run, omitting the substrate from the reaction mixture.

## RESULTS

***Floral organography***—Flowers of *P. sagittata* are moderately zygomorphic and vary in color from pale lilac to light purple. A prominent yellow nectar guide is present on the up-

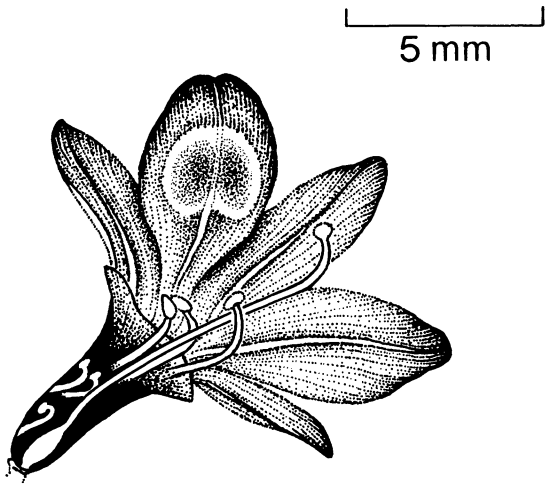


Fig. 1. A flower of the long-styled morph of *Pontederia sagittata.*

per middle tepal. The flower is composed of six tepals that arise in two alternate, trimerous whorls. Tepals are fused for over half their lengths to form a perianth tube. Flowers are hypogynous and have two stamen sets consisting of three stamens each (Fig. 1). The anthesis period of individual flowers is six to eight hr with no apparent differences in the timing of sexual function (dichogamy) between male and female organs.

The general features of the tristylous floral polymorphism in *P. sagittata* can be briefly summarized. Reproductive organs are positioned at three distinct levels within the floral morphs designated as the long-, mid-, and short-levels. These levels correspond to the height of the anthers of the two stamen sets (Fig. 2) and to the height of the stigma above the base of the flower. In each floral morph the stigma occupies the level not occupied by the two anther sets. Thus the long-styled morph (L) has a long style and mid- (m) and short- (s) level anthers, the mid-styled morph (M) has a mid-length style and long- (l) and short- (s) level anthers, and the short-styled morph (S) has a short style and mid- (m) and long- (l) level anthers. Quantitative descriptions of the polymorphism are detailed below. Figure 3 illustrates schematically important features of the pollen tube pathway.

***Androecial characters***—With reference to level (height above the base of the ovary), each floral morph has an upper and a lower stamen set composed of three stamens. In relation to the dorsiventrality of the flower, the lower stamen set is inserted on the adaxial three tepals of the perianth, while the upper stamen set is inserted on the abaxial three tepals (Fig. 2). Since the tepals and stamens within a flower arise sequentially in four alternate and trimerous whorls, upper-level stamens are composed of two stamens of the outer stamen whorl and one of the inner stamen whorl. Lower-level stamens are composed of two stamens of the inner whorl, and one of the outer whorl (Fig. 2). A feature of this arrangement is that long- and short-level stamens are always inserted on the abaxial and adaxial tepals, respectively. In contrast, mid-level stamens have a heterogeneous origin being inserted on the abaxial tepals of the flower in the L morph but on the adaxial tepals in the S morph.

Height of the central anther (sum of floral tube, filament, and anther length) within all lower-level stamen sets is less than that of anthers of the outer stamens. In upper-level stamens the reverse pattern occurs (Fig. 2). Differences in anther height among stamens within lower stamen sets are mainly attributable to differences in floral tube length (distance between base of ovary and base of free filament of the stamen). This is not the case in upper stamens. Comparisons of pooled floral tube lengths by stamen set indicates that stamen sets fall into two groups corresponding to whether a stamen is the upper or lower set within a floral morph.

In contrast to floral tube length, stamen filament length (Fig. 2) and anther length (Table 1) separate into the three classes corresponding to the three stamen levels characteristic of the tristylous floral syndrome (Fig. 2). There is a tendency for filaments of the central stamen to be slightly longer than filaments of the outer stamens in all stamen sets although these differences are not statistically significant. Anther width does not vary significantly between stamen levels (Table 1).

Pollen of the three anther levels shows a marked size trimorphism. Pollen from l anthers is largest, pollen from s anthers is smallest, and pollen from m anthers is of intermediate size (Figs. 4–6). Pollen is binucleate, disulcate, and minutely reticulate. Unlike the pollen of many distylous plants, conspicuous differences in exine reticulations between the pollen types were not evident. All three pollen types stain positively for starch.

***Gynoecial characters***—Differences between the gynoecia of the floral morphs are presented in Table 2; the most characteristic difference is in the style length. Comparisons indicate that styles of the L morph are 12 times, and the M morph are six times the length of styles of the S morph, respectively. Variation in stigma height (style length plus ovary length) results from differences in style length alone, since

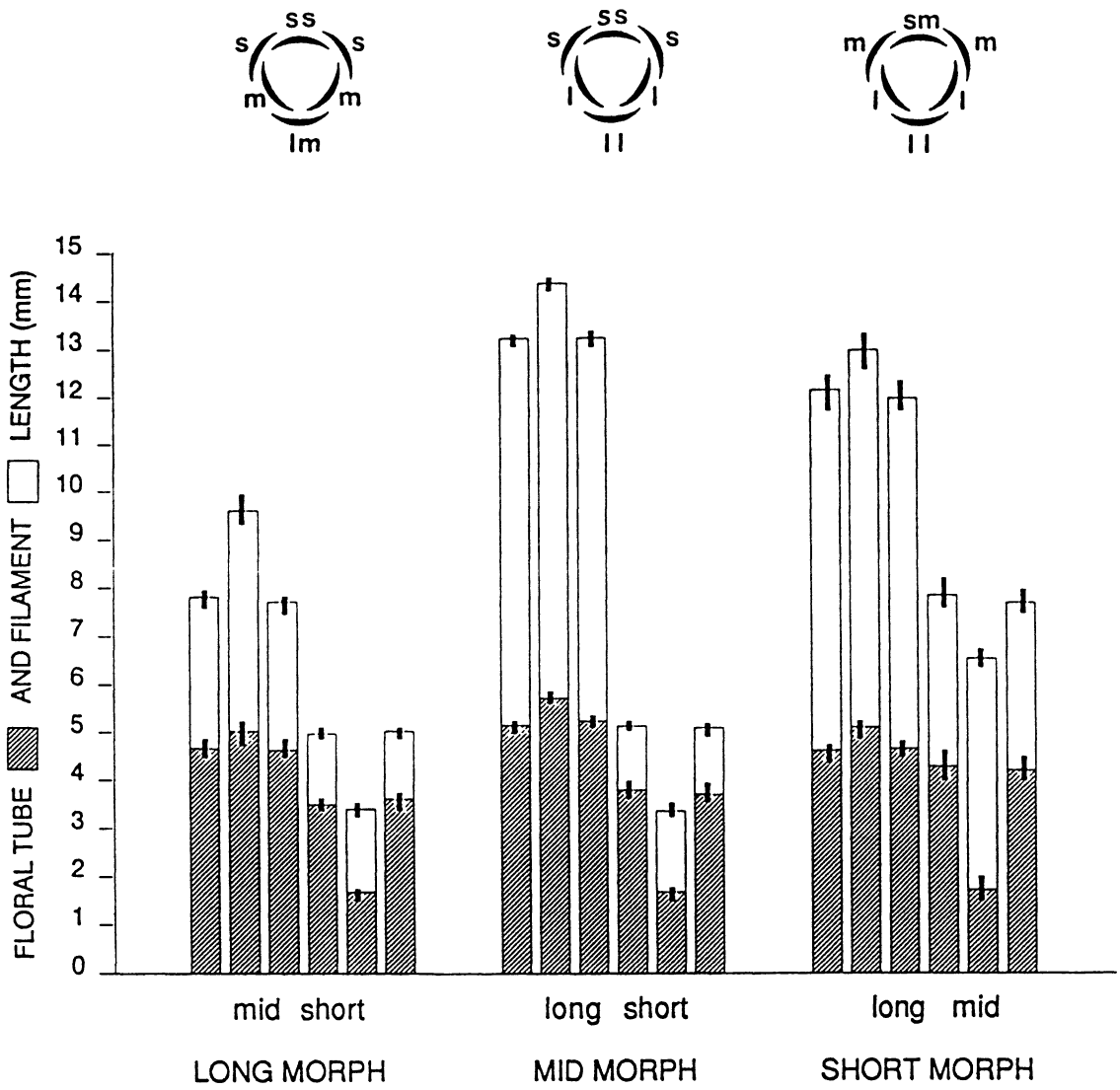


Fig. 2. Diagram of average floral tube (shaded) and filament (unshaded) lengths for the three stamens of each stamen level within the floral morphs. Anther height is the sum of floral tube and filament length. The left bars represent the three upper stamens (inserted abaxially), and the right bars represent the three lower stamens (inserted adaxially) in each floral morph. Each mean is based on measurement of 30 stamens. Error bars represent 95% confidence intervals. Means and standard deviations for floral tube and filament lengths are given in Tables 2 and 3, respectively. Diagrams above the histograms for each floral morph indicate the tepal with which each stamen is associated. Each upper stamen level has a central longer stamen (ll or lm), while each lower stamen level has a central shorter stamen (ss or sm).

ovary length does not vary significantly among the floral morphs (Table 2). Stylar cell length differs among the floral morphs, with S styles having the shortest cells, L styles the longest, and M styles having intermediate cell lengths (Table 2). When ratios of stylar cell length are compared between the floral morphs, however, the ratio of cell lengths is far less than that for style length, indicating that an increase in cell number must also contribute to the observed differences.

Stigmas of the floral morphs are formed by outgrowth of the epidermal cells at the tip of each lobe of the style (Figs. 7–9). At the commencement of anthesis the three major stigmatic lobes (each major lobe being subdivided into two minor lobes) are closely appressed so that individual lobes are not readily visible (arrow, Figs. 7–9). As anthesis progresses, separation and elongation of the stigmatic lobes occurs such that each lobe is visibly subdivided into two smaller lobes. Four of the six minor stigmatic lobes of the style of the L morph are visible in Fig. 15. Stigma depth in the L morph

TABLE 1. *Mean length and width (mm) ± standard deviation of anthers in the floral morphs of* Pontederia sagittata. *After a two-way ANOVA, means were compared using Scheffe's method. Uppercase superscripts refer to comparisons among anther lengths, lowercase superscripts refer to comparisons among anther widths. Means sharing the same superscript are not significantly different (P > 0.05; N = 30)*

| | Floral morph | | | | | | | |
|---|---|---|---|---|---|---|---|---|
| | Long | | Mid | | Short | | | |
| Anther level | Length | Width | Length | Width | Length | Width | | |
| Long | — | | $1.06^{A} \pm 0.097$ | $0.478^{a} \pm 0.107$ | $0.906^{B} \pm 0.089$ | $0.397^{b} \pm 0.063$ | | |
| Mid | $0.815^{C} \pm 0.088$ | $0.385^{b} \pm 0.094$ | — | | $0.827^{C} \pm 0.089$ | $0.430^{b} \pm 0.070$ | | |
| Short | $0.738^{D} \pm 0.104$ | $0.432^{b} \pm 0.114$ | $0.750^{D} \pm 0.059$ | $0.424^{b} \pm 0.052$ | — | | | |

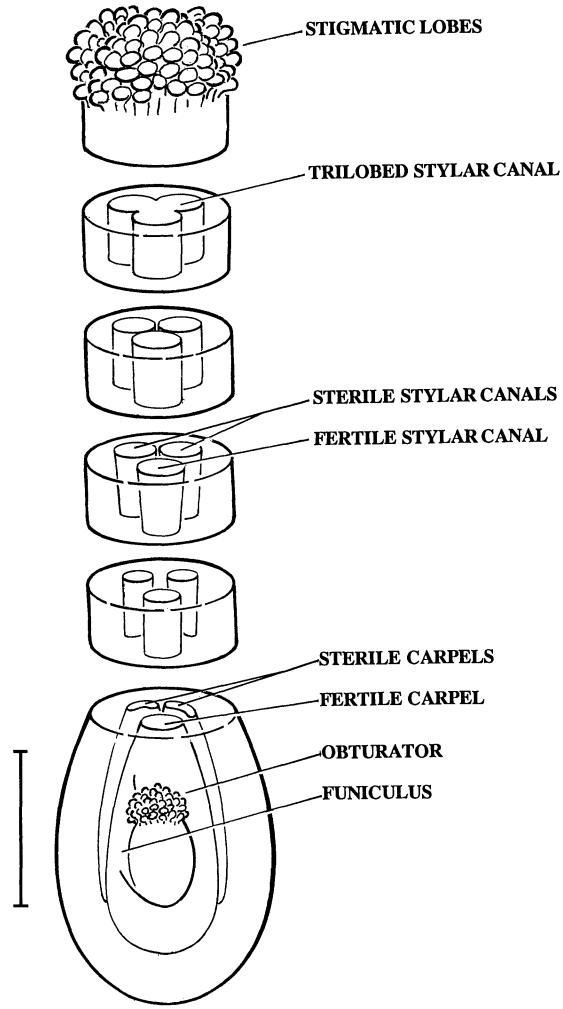


Fig. 3. Schematic diagram of the pistil of *Pontederia sagittata* showing important features of the pollen tube pathway. Note the separation of the trilobed stylar canal into two sterile canals of reduced area (leading to sterile carpels) and a single fertile canal opening into a fertile carpel. Bar = 1 mm.

is almost twice that of the M morph, and is five times that of the S morph (Table 2). There is an increase in number of stigmatic papillae from the S to M to L morph (Figs. 7–9). Length of stigmatic papillae varies significantly between the floral morphs, increasing with increasing style length (Table 2; Figs. 10–12). Stigmatic papillae are capitate in shape, with this shape becoming more pronounced from the S to M to L morph.

***Stigmatic cytochemistry***—No major differences in cytochemistry of the stigma surface were revealed between the floral morphs. As a result, the following descriptions apply to all morphs. For consistency, all micrographs

TABLE 2. *Mean organ length and cell size with standard deviation for the gynoecium in the floral morphs of* Pontederia sagittata. *After a Kruskal-Wallis test, ranks were compared using Dunn's multiple comparisons procedure. Means sharing the same superscript are not significantly different ($P > 0.05$; $N = 30$ for all variables except papillae length, $N = 300$ and stylar cell length, $N = 600$)*

| | Floral morph | | |
|---|---|---|---|
| | Long | Mid | Short |
| Style length[b] | $12.21^{A} \pm 0.80$ | $6.00^{B} \pm 1.91$ | $1.00^{C} \pm 0.22$ |
| Stylar cell length[a] | $108.32^{A} \pm 13.78$ | $93.52^{B} \pm 14.75$ | $50.68^{C} \pm 10.12$ |
| Stigma depth[a] | $328.40^{A} \pm 15.14$ | $184.42^{B} \pm 6.90$ | $77.00^{C} \pm 8.32$ |
| Papilla length[a] | $173.12^{A} \pm 21.56$ | $157.67^{B} \pm 19.36$ | $136.87^{C} \pm 16.87$ |
| Ovary length[b] | $1.99^{A} \pm 0.18$ | $1.93^{A} \pm 0.10$ | $1.92^{A} \pm 0.50$ |
| Ratio of style to cell length | 112.72 | 64.16 | 19.73 |
| Ratio of style length | 12.21 | 6.00 | 1.00 |
| Ratio of cell length | 2.14 | 1.85 | 1.00 |

[a] In μm.
[b] In mm.

showing cytochemical features are of the L morph.

Large numbers of plastids are present in stigmatic cells and in upper regions of the style (Figs. 14, 15). Based on starch staining, these appear to be amyloplasts, showing a negligible affinity for protein staining with Coomassie blue (Fig. 16, arrow), and lipid staining with both phosphine (Fig. 18) and Sudan III (Fig. 21).

Toluidine blue staining suggests that there is a strong carbohydrate component in the cytoplasm (Fig. 27). The cytoplasm of the stigmatic papilla in Fig. 18 (arrow) is visible after phosphine staining for lipids and has pulled away from the cell wall. The cell wall is particularly evident after alcian blue staining for pectic polysaccharides (Fig. 26, small arrow) and toluidine blue staining for carbohydrates (Fig. 27, small arrow). The stigmatic papillae are bound by a cuticular layer which is readily identified by its intense staining for cutin with auramine O (Fig. 20). A thin pellicle forms a fine layer over the surface of the cuticle and stains strongly for proteins with 1-ANS (Fig. 17, small arrows). The high reactivity of this layer with nonspecific esterase is its most distinguishing feature (Fig. 28). Control stigmas

→

Figs. 4–14. Structural features of floral heteromorphisms. Figs. 4–12. SEM micrographs. Figs. 13, 14. LM micrographs. Figs. 4–6. Pollen from the three stamen levels. Notes the size decrease in pollen from the long- to mid- to short-level anther and the absence of exine sculpturing differences between the pollen types. Bars = 20 μm. **4.** Long-level anther pollen. **5.** Mid-level anther pollen. **6.** Short-level anther pollen. Figs. 7–9. Stigmas of the three floral morphs. Note the decrease in stigma size from the L to M to S morph. Bars = 20 μm. **7.** L morph. **8.** M morph. Note the suture between two lobes of the style (arrow). **9.** S morph. Note the close positioning of adjacent stigma lobes (large arrow) and the suture between two of the lobes of the style (small arrow). Figs. 10–12. Stigmatic papillae of the three floral morphs. Note the decrease in size of the papillae from the L to M to S morph. Bars = 10 μm. **10.** L morph. **11.** M morph. **12.** S morph. **13.** Longitudinal section of a stigma of the L morph. Note the stigmatic papillae formed by an outgrowth of epidermal cells of the style. Exudate is visible on the stigmatic papillae (arrows). Note that the stylar canal opens directly onto the stigma, and that secretory cells line the stylar canal to the tip of the inner face of the stigma (arrowhead). Bar = 10 μm. **14.** Iodine-potassium iodide (IKI) staining for starch in the stigmatic papillae of the L morph. Note the prominent amyloplasts in the cytoplasm of the stigmatic papillae (arrows). Bar = 10 μm.

Figs. 15–26. Stigmatic cytochemistry. Figs. 15–26. LM micrographs. Cytochemistry of the stigma surface of the L morph. **15.** IKI staining for starch. Note the high density of amyloplasts in the four stigmatic lobes. Bar = 20 μm. **16.** Coomassie blue staining for proteins. Note the absence of staining of amyloplasts (arrow) and the staining of exudate both on the stigma surface and cuticle (arrowheads). Bar = 10 μm. **17.** 1-ANS staining for proteins (UV light). Note the intense staining of the cuticle surface for proteins (arrows). Bar = 10 μm. Figs. 18, 19. Phosphine staining for lipids. Bars = 10 μm. **18.** White light. The arrow indicates the cytoplasm of a stigmatic papilla which is separated from the cell wall. **19.** Same stigma as shown in Fig. 18 viewed under UV light. Note the staining of the cuticle (arrows) on the sides of the papillae but not at the tip. **20.** Auramine O staining for lipids. Note the intense staining of the cuticle and presence of droplets of exudate (arrows). Bar = 10 μm. Figs. 21, 22. Sudan III staining for lipids. Bars = 10 μm. **21.** White light. Note exudate staining (arrowheads). **22.** UV illumination of the stigma shown in Fig. 21. Note the quenching of cuticular staining (arrows) and the exudate at the base of the stigma (arrowhead). **23.** Nile blue staining for lipids. Note the thinning of the cuticle toward the tip (arrows). Bar = 10 μm. **24.** Sudan black staining for lipids (UV light). Note the quenching of staining in the area between the cell wall and cuticle (arrows). Bar = 10 μm. **25.** Unstained control stigma viewed under UV illumination. Note the weak autofluorescence of the cuticle. Bar = 10 μm. **26.** Alcian blue staining for pectic polysaccharides. Note the distinct staining of the pectocellulosic cell wall (arrows). Exudate is visible on the stigma surface as a thin layer (arrowheads). Bar = 10 μm.

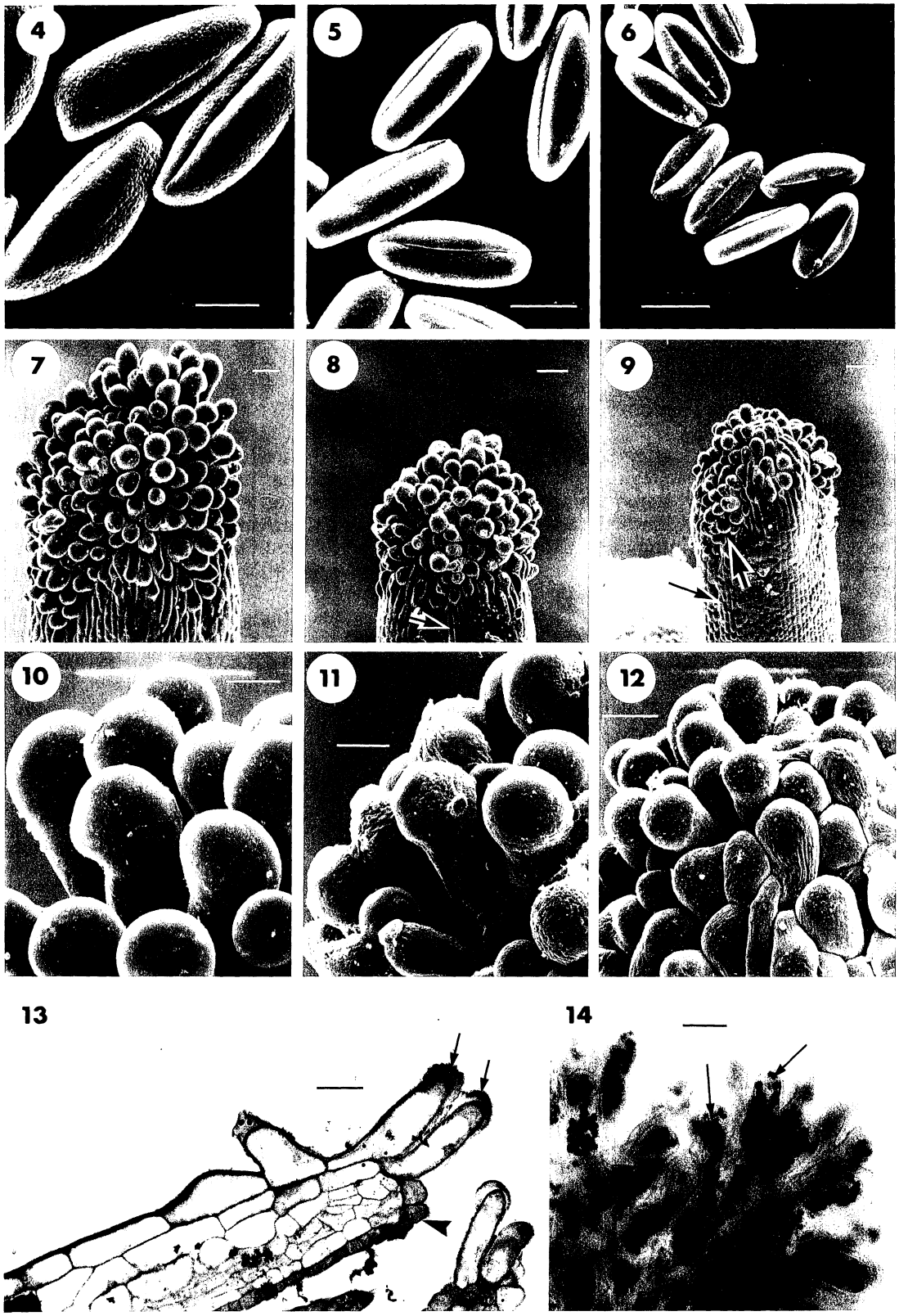
4
5
6
7
8
9
10
11
12
13
14


15


16

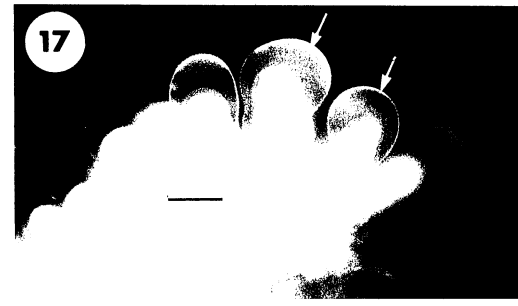
17

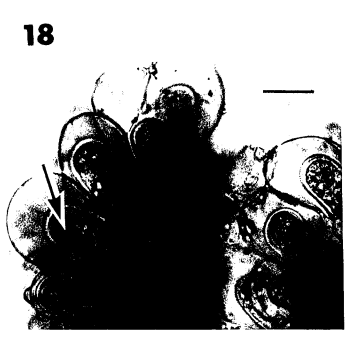
18

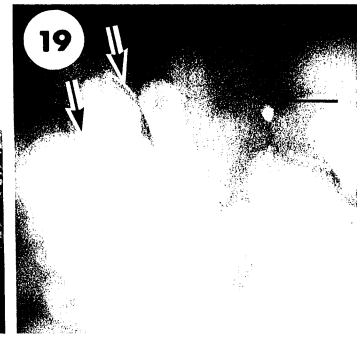
19

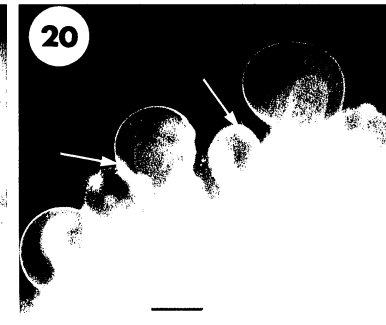
20

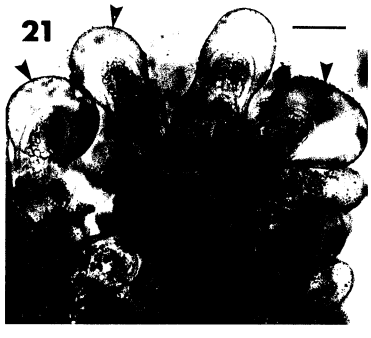
21

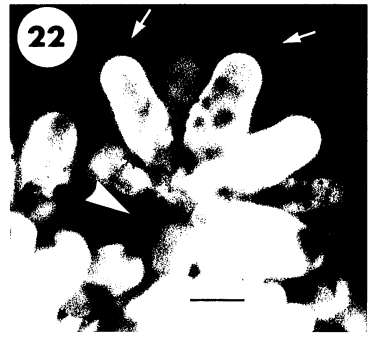
22

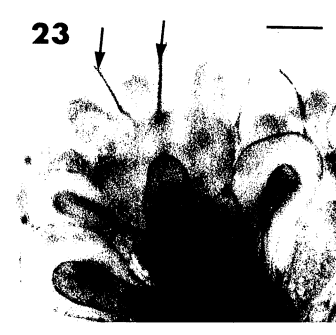
23

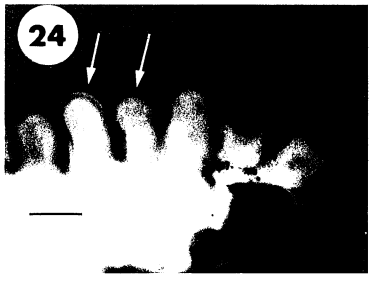
24

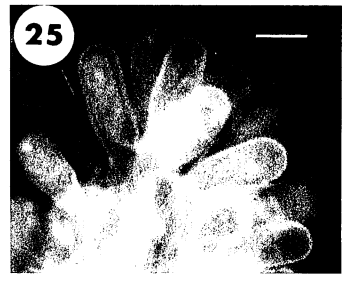
25

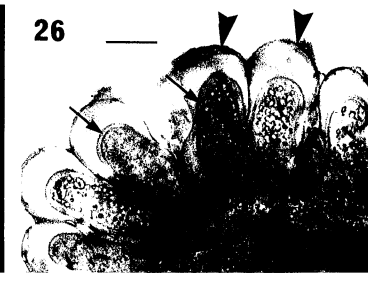
26

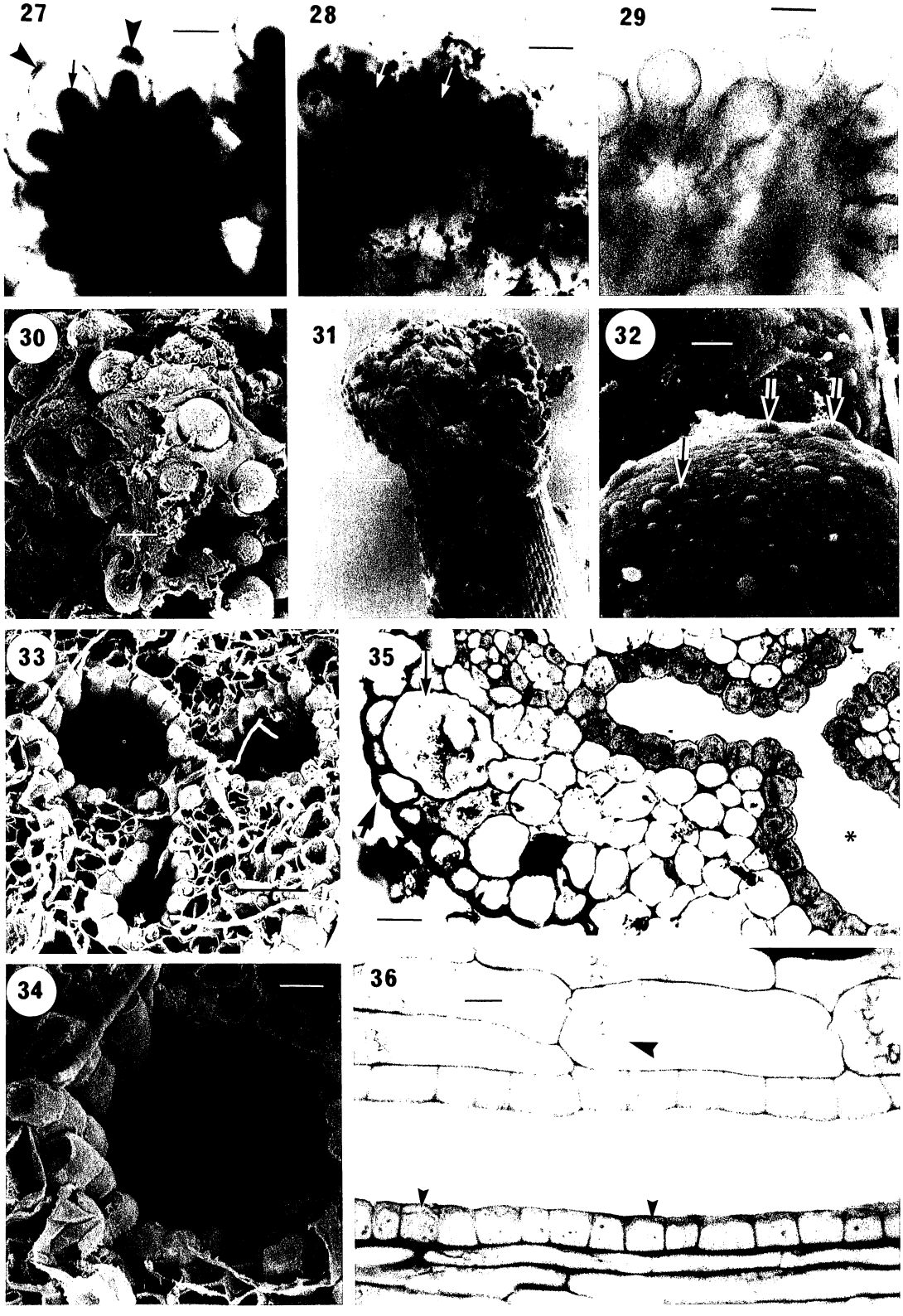
27
28
29
30
31
32
33
35
34
36

show no staining (Fig. 29). The fragmented appearance of the pellicle in Fig. 28 is the result of damage associated with preparation of stigmas for microscopy. This layer is continuous in intact papillae.

At the beginning of anthesis little to no exudate is visible on the stigma surface (Figs. 7–12). Later in anthesis copious exudate becomes obvious, particularly on stigmas of the L morph (Fig. 30) where it often flows over the stigma and down the epidermis of the style (Fig. 31). The degree of exudate accumulation decreases from the L to M to S morph. In the S morph in particular, only small droplets are visible on the stigmatic papillae (Fig. 32, arrow), and the stigma never appears wet.

Stigmatic papillae become more capitate in appearance as anthesis progresses, apparently resulting from the accumulation of material between the cuticle and underlying pectocellulosic cell wall (compare Fig. 13 with Figs. 10, 17–27). As accumulation occurs the cuticle lifts away from the underlying cell wall, resulting in swelling at the tips of the stigmatic papillae. The accumulated material stains distinctly with Sudan black for lipids which is indicated by strong quenching under UV illumination (Fig. 24, arrows).

Droplets present on the stigma surface (Fig. 32) may represent exudates originating from the stylar canal or material that has been secreted across the cuticle of the stigmatic papillae. Transmission electron microscopy studies would be required to determine the nature of the secretory process in stigmatic papillae. Exudate droplets stain strongly for lipids with auramine O (Fig. 20, arrows) and for carbohydrates with both alcian blue (Fig. 26) and toluidine blue (Fig. 27). A thin layer of exudate over the papillae is particularly evident with alcian blue staining for pectic polysaccharides (Fig. 26, large arrows) and toluidine blue for carbohydrates (Fig. 27, large arrows). Staining for lipids with phosphine and Nile blue indicates that the cuticle thins at the tips of the stigmatic papillae (Figs. 19, 23, between the arrows).

In addition to droplets and layering on the stigma surface, large quantities of additional exudate collect between adjacent papillae and stigma lobes. This exudate stains strongly for lipids with Sudan III (Fig. 22, large arrow) and for proteins with Coomassie blue (Fig. 16, large arrows).

***Stylar anatomy***—At the stigma base the stigmatic lobes join to form a trilobed style. Each lobe is separated by a distinct suture that runs the length of the style (Figs. 8, 9, small arrow). The shape of the style does not vary between the morphs. A hollow trilobed canal is present in the central part of the style (Figs. 33–35, 37), each lobe of the stylar canal corresponding to a carpel in the ovary. Figure 3 is a schematic illustration showing structural features of the pistil of *P. sagittata* that are important components of the pollen tube pathway.

Cells of the cortical region of the style are typical parenchyma cells with a large central vacuole and a thin layer of cytoplasm immediately beneath the cell walls. These parenchyma cells appear circular in transverse section (Fig. 34) and rectangular in longitudinal view (Fig. 36) and contain amyloplasts (Fig. 36, large arrow). Crystal idioblasts are common in the peripheral parenchyma cell layers immediately beneath the epidermis (Fig. 34, small arrow) and most commonly contain large raphide bundles (Figs. 38, 39). The epidermis of the style has a thick cuticle (Fig. 34, large arrow).

The stylar canal is lined by specialized cells with much smaller dimensions than stylar parenchyma cells, particularly as seen in longi-

←

Figs. 27–36. Stigmatic cytochemistry and stylar anatomy. Figs. 27–29, 35, 36. LM micrographs. Figs. 30–34, 35. SEM micrographs. Figs. 27–29. Stigma cytochemistry. Bar = 10 μm. **27.** TBO staining for carbohydrates. Note the staining of the cell wall (arrow) of the papillae and the staining of the exudate (arrowheads). **28.** Nonspecific esterase staining of the pellicle (arrows). The fragmented appearance of the pellicle is an artifact of specimen preparation. **29.** Control for the esterase reaction. Note the absence of staining. **30.** Exudate accumulation on the stigmatic papillae of the L morph. Bar = 20 μm. **31.** Copious exudate on the stigma of the L morph. Bar = 50 μm. **32.** Higher magnification view of the surface of a stigmatic papilla of the S morph showing the formation of exudate droplets (arrows). Bar = 1 μm. **33.** Transverse view of the trilobed stylar canal. Note the specialized cells lining the stylar canal. At this level the trilobed stylar canal is just forming three separate stylar canals. Bar = 20 μm. **34.** Higher magnification view of the style from Fig. 33. Note the close packing of cells in the stylar canal and their domed secretory face. Bar = 5 μm. **35.** Transverse section of the style just below the stigma. Toluidine blue staining. Note the trilobed shape of the stylar canal, dense staining of the secretory cells lining the stylar canal, staining of exudate on the surface of the stylar canal cells (asterisk), crystal idioblast (arrow) in the peripheral layers of the stylar cortex, and the thickened walls of cells of the stylar epidermis (arrowhead). Bar = 10 μm. **36.** Longitudinal section through the stylar canal stained with toluidine blue showing details of the stylar canal cells. Note the size, shape, and staining density of stylar canal cells in comparison with stylar parenchyma cells. Exudate is visible on the secretory face of the stylar canal cells (small arrowheads). Note the amyloplasts in the parenchyma cells (large arrowhead). Bar = 5 μm.

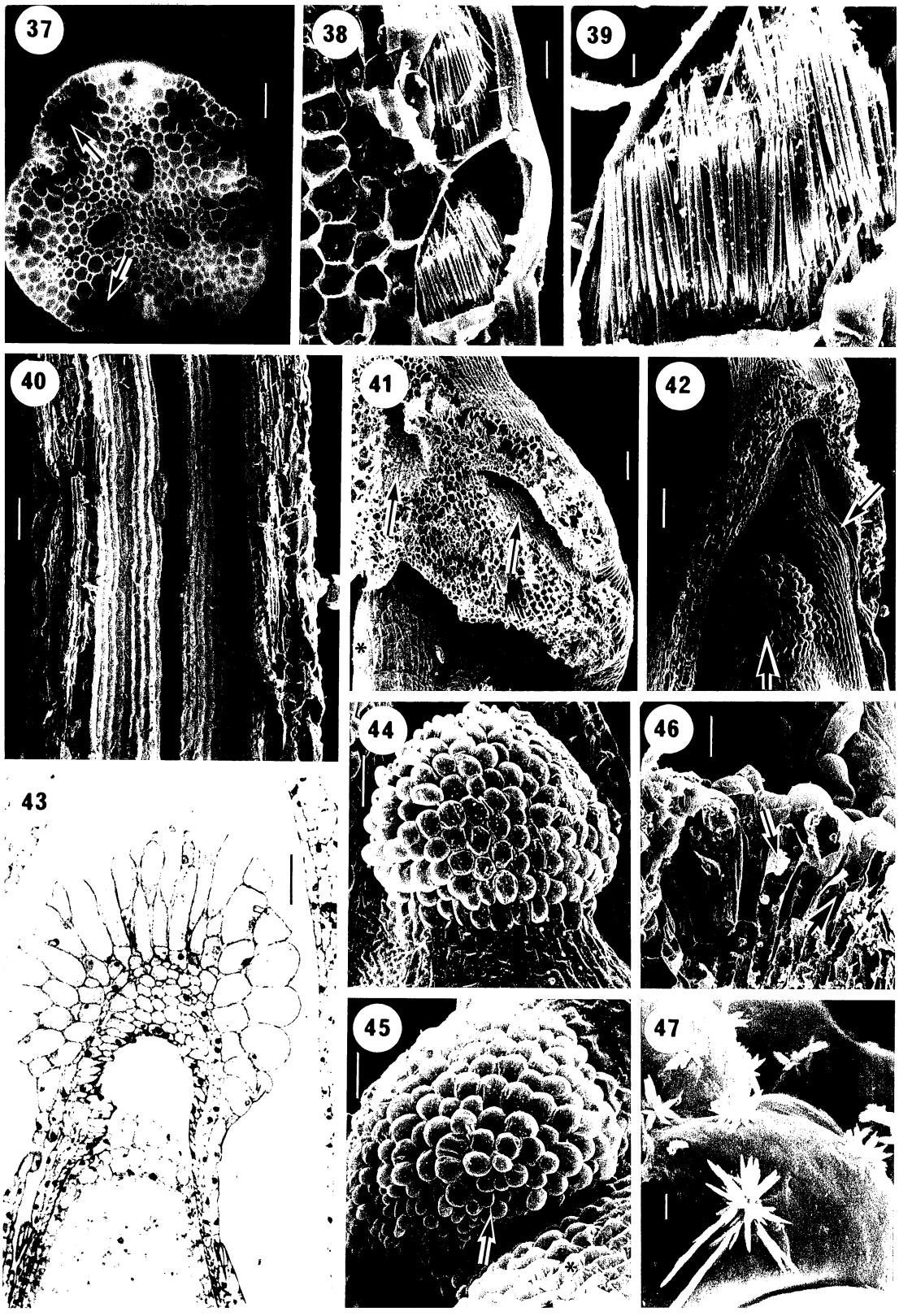
37
38
39
40
41
42
43
44
45
46
47

TABLE 3. *Mean cross-sectional area ($mm^2 \times 10^{-3}$) of style and stylar canal (total) and standard deviation at the top, middle, and base of the style in the floral morphs of* Pontederia sagittata. *After a two-way ANOVA, means were compared using Scheffe's method. Data were square root-transformed prior to analysis. Uppercase superscripts refer to comparisons among stylar areas, lowercase superscripts refer to comparisons among stylar canal areas. Means sharing the same superscript are not significantly different ($P > 0.05$; $N = 30$ styles)*

| Level | | Floral morph | | |
|---|---|---|---|---|
| | | Long | Mid | Short |
| Top | Style | $107.47^{A} \pm 14.72$ | $77.67^{BC} \pm 9.03$ | $41.25^{D} \pm 6.98$ |
| | Canal | $12.32^{a} \pm 2.36$ | $11.14^{a} \pm 2.16$ | $6.27^{d} \pm 0.92$ |
| Mid | Style | $113.49^{A} \pm 13.28$ | $80.24^{B} \pm 12.15$ | $51.00^{D} \pm 12.09$ |
| | Canal | $11.13^{a} \pm 1.35$ | $9.05^{b} \pm 1.38$ | $6.79^{cd} \pm 1.69$ |
| Base | Style | $82.26^{B} \pm 9.52$ | $79.29^{B} \pm 9.86$ | $66.03^{C} \pm 19.72$ |
| | Canal | $9.12^{b} \pm 2.09$ | $9.05^{b} \pm 1.61$ | $8.24^{bc} \pm 1.71$ |

tudinal section (Fig. 34). The canal cells are often domed on their secretory face (Figs. 35, 36) with a dense cytoplasm and thick cell wall (Figs. 34, 36). Canal cells line the stylar canal for the entire length of the style (Fig. 40) up to its entry point into the ovary but do not line the ovary cavity. They also extend to the tip of the inner face of the stigma (Fig. 13, large arrow).

Stylar canal cells appear to be secretory in function (Fig. 36, small arrows). The toluidine blue staining in this micrograph indicates that the exudate has a carbohydrate component. Since styles examined for structural features of the stylar canal were collected early in the day, little exudate is visible in the stylar canal of the micrographs. As exudate accumulation continues throughout the day these secretions fill the stylar canal (asterisk, Fig. 35), often welling up onto the stigma surface and flowing over the epidermis of the style in the L morph (Fig. 31).

Data on cross-sectional area of the style and stylar canals (sums of areas of the three individual canals) for the three morphs at the three levels in the style are shown in Table 3. Comparisons of style area between the floral morphs at the top and middle of the style indicate that area increases from the S to M to L morph. At the base of the style, area is not significantly different between the L and M morphs, but is significantly greater than the S morph. Average style area values for the morphs indicate that style area of the L morph is 1.9 times, and the area of the M morph is 1.5 times, that of the S morph.

Comparisons of total stylar canal area in the morphs indicate that canal area is significantly different between the S morph, and the L and M morph at the top of the style, among all three morphs at the midpoint in the style, and is not significantly different among the morphs at the base of the style. Comparisons of stylar canal area with total style area show that the proportion of the style occupied by stylar canal increases from the L to M to S morph for all levels in the style (Table 3).

In all sections examined, stylar canals were always trilobed at the top of the style (Fig. 35). In the L and M morph the canal branched into three separate ellipsoidal canals by the mid-level in all styles examined ($N = 30$) (Figs. 3, 33, 37). In the S morph, however, in 11 of 30 styles sampled the stylar canal was still trilobed

←

Figs. 37–47. Stylar and ovular structure. Figs. 37, 43. LM micrographs. Figs. 38–42, 44–47. SEM micrographs. **37.** Transverse section at the base of the style. Aniline blue staining for callose. Note the reduced area of the lower two sterile stylar canals compared with the upper fertile stylar canal and tannin cells in the peripheral layers of the stylar cortex (arrows). Bar = 20 μm. **38.** Longitudinal view of crystal idioblasts in the peripheral layers of the stylar cortex just beneath the epidermis. Bar = 5 μm. **39.** Higher magnification view of Fig. 38. Bar = 1 μm. **40.** Longitudinal section of the style showing the surface of two of the stylar canals ×300. Bar = 20 μm. **41.** Transverse sectional view of the two sterile stylar canals (arrows) near the top of the ovary. The fertile stylar canal is continuous with the ovary cavity. The funiculus of the ovule is visible on the left (asterisk). The style is toward the top of the micrograph. Bar = 20 μm. **42.** Longitudinally sectioned view of the ovary. The ovule is anatropous with the funiculus attached at the base of the style (top of micrograph). Note the obturator of the ovule (large arrow). Note the pollen tubes (small arrow) entering the ovary cavity onto the surface of the funiculus at a point opposite the obturator. Bar = 50 μm. **43.** Longitudinal section of the obturator. The obturator is an outgrowth of the outer integument. Note the elongated and papillate cells that make up the surface of this structure. Bar = 20 μm. **44.** Side view of the obturator showing its papillate morphology. Bar = 20 μm. **45.** Top view of the obturator. Note the decrease in size of the papillae close to the funiculus (asterisk). Bar = 20 μm. **46.** Longitudinal section through the papillae of the obturator. Note the thin cell walls (small arrow) and amyloplasts (large arrow). Note the four pollen tubes approaching the obturator at the top of the micrograph. Bar = 10 μm. **47.** Druse crystals on the surface of the papillae of the obturator. Bar = 1.0 μm.

TABLE 4. *Mean cross-sectional area ($mm^2 \times 10^{-3}$) of fertile and sterile stylar canals and standard deviation at the middle and base of the style in the floral morphs of* Pontederia sagittata. *After a two-way ANOVA, means were compared using Scheffe's method. Data were log-transformed prior to analysis. All possible comparisons are shown. Means sharing the same superscript are not significantly different ($P > 0.05$; $N = 30$ except for mid-level canal areas in the Short morph, $N = 19$)*

| Level | | Floral morph | | |
|---|---|---|---|---|
| | | Long | Mid | Short |
| Mid | Fertile | $5.20^{A} \pm 1.11$ | $4.34^{A} \pm 0.89$ | $2.65^{BC} \pm 0.53$ |
| | Sterile | $2.96^{C} \pm 0.54$ | $2.34^{BC} \pm 0.48$ | $1.63^{B} \pm 0.50$ |
| Base | Fertile | $4.59^{A} \pm 1.44$ | $4.99^{A} \pm 0.99$ | $4.56^{A} \pm 1.31$ |
| | Sterile | $2.27^{BC} \pm 0.56$ | $2.03^{B} \pm 0.52$ | $1.84^{B} \pm 0.50$ |

at the midpoint of the style. Three separate canals were present at the base of the style in all styles of the three morphs. Only one of the three stylar canals leads to a fertile carpel containing the single ovule. The other two canals lead to sterile carpels (Figs. 3, 41, 42).

Data for areas of individual stylar canals is shown in Table 4. Values are only shown for the middle and base of the style since the stylar canal is trilobed and not divided into separate canals at the top of the style. The data indicate that fertile stylar canals have approximately 1.7 times the area of a sterile stylar canal at the midlevel in the style in all of the morphs and that this ratio increases to two times in the L morph and 2.5 times in the M and S morphs at the base of the style. Comparing canal area within a level among the morphs indicates that at the midlevel in the style, fertile canal areas of the L and M morph are not significantly different, but are greater in area than the S morph. This is also the case for sterile canals. At the base of the style there are no significant differences when comparing fertile canal areas, or when comparing sterile canal areas among the morphs.

***Ovarian anatomy***—Sterile stylar canals open into vestigial carpels in the ovary. These narrow carpels are restricted to the peripheral region of the ovary (Fig. 41, arrows), the majority of the ovary being occupied by the fertile carpel (Fig. 42). The single fertile carpel bears an anatropous ovule with its funicular attachment just below the point where the fertile stylar canal opens into the ovary (Fig. 42). The point of entry is opposite to the position of the obturator. This can be seen clearly in Fig. 42 where pollen tubes (large arrow) have grown into the ovary cavity down the abaxial face of the funiculus.

The most prominent feature of the ovule is an obturator (Fig. 42, arrow) formed as an outgrowth of the outer integument (Figs. 43–45). The papillae of the obturator are not of uniform size, becoming smaller where the obturator is appressed to the funiculus (Fig. 45, arrow). The papillae are thin walled (Fig. 43; Fig. 46, small arrow) and contain numerous amyloplasts (Fig. 46, large arrow). The papillae commonly have druse-shaped crystals on their surfaces although the anatomy of the papillae is not suggestive of cells having a secretory function (Fig. 47). No differences were observed between the morphs in either ovule or obturator size or structure.

As in the style, ovarian tissue contains large numbers of crystals. These are in the form of raphide bundles, as well as styloid and prismatic crystals. Although some of these are idioblastic in nature, many also appear to be free in the ovary cavity.

## DISCUSSION

To assess the functional role of heteromorphic characters in pollen-pistil interactions of heterostylous plants, information on their morphological and anatomical features is required. The major goal of this study was to provide a detailed description of androecial and gynoecial characters in tristylous *P. sagittata* so that subsequent investigations of pollen tube growth could be interpreted within a structural context (Scribailo and Barrett, 1991).

Several of the floral heteromorphisms in *P. sagittata* (e.g., pollen size, pollen production, style length, anther height) are near ubiquitous in other heterostylous families (Ganders, 1979). Their widespread occurrence suggests that they play an integral role in the functioning of heterostyly (Dulberger, 1975b). In contrast, heteromorphisms involving conspicuous exine sculpturing that are common in distylous taxa are absent in *P. sagittata,* while others (e.g., stamen arrangement and stylar canal traits) exhibit distinctive patterns of expression. The occurrence or particular expression exhibited by heteromorphic characters in a given group will be strongly influenced by its evolutionary history. Phylogenetic constraints on the evolution of heteromorphic characters are of par-

ticular interest in the Pontederiaceae owing to the isolated occurrence of heterostyly in the monocotyledons. The only additional taxa known to be heterostylous within the monocotyledons are *Nivenia* (Mulcahy, 1965) and *Narcissus* (Lloyd, Webb, and Dulberger, 1990), both of which exhibit atypical heterostylous features. Because of this, functional interpretations of heteromorphic characters in *P. sagittata* may be more informative if they are undertaken within a phylogenetic framework, taking into account the likely reproductive characteristics of their nonheterostylous monocotyledonous ancestors (see Eckenwalder and Barrett, 1986).

Several findings from this study are in accord with earlier investigations of the tristylous syndrome in the Pontederiaceae (e.g., Price and Barrett, 1982; Glover and Barrett, 1983; Richards and Barrett, 1984, 1987). Of particular interest is the pattern of variation in stamen height that occurs within and between stamen levels. This pattern results from imposition of a dorsiventral symmetry in stamen arrangement on a flower with typical monocotyledonous development with radial symmetry and parts arranged in trimerous whorls. Richards and Barrett (1984, 1987) have discussed some of the developmental consequences of these patterns which appear to be unique to heterostyly in the Pontederiaceae.

Lower-level stamens in *P. sagittata* are associated with a pronounced difference in floral tube length between central and outer stamens, while in upper-level stamens this difference is less well developed. Although the observed differences in floral tube length are probably a function of the heterogeneous origin of stamens within a stamen level (with stamens originating from both outer and inner tepal whorls), why such marked differences should be present between upper- and lower-level stamens is unclear.

Floral tube lengths compared between stamen sets separate into two groups corresponding to whether a stamen is in the upper- or lower-level within a flower. In contrast, stamen filament lengths separate into three distinct groups corresponding to the three stamen levels associated with tristyly. These differences are suggestive that the expression of stamen trimorphism originates primarily through differential elongation of filaments. This observation, as well as heterogeneity between stamens within a level, indicates that at least some components of tristyly may be expressed relatively late in floral development (see Richards and Barrett, 1984, 1987). The observed differences are interesting from a functional perspective because of Dulberger's (1975b) suggestion that differential elongation of floral parts may be involved in the production of incompatibility specificities.

Increases in stigma depth and stigmatic papillae length from the S to M to L morph are correlated with the style length trimorphism and are manifestations of both increased cell number and greater cell extension in longer styles. Morph-specific differences in stigmatic papillae length in conjunction with pollen size and pollen exine heteromorphisms are thought to be of importance in distylous taxa in promoting the preferential adhesion, hydration, and germination of legitimate pollen (see Gibbs, 1986).

Several studies have suggested that stigma depth may be an important isolating mechanism in interspecific crosses (Plitman and Levin, 1983; Cruden and Lyons, 1985). Observations on pollen tube growth in *P. sagittata* suggest that stigma depth may in part act in a similar fashion in illegitimate pollinations (Scribailo and Barrett, 1991).

Smith (1898) reported the presence of a hollow stylar canal in *P. cordata,* and the presence of such a canal is also shown here for *P. sagittata.* The analysis of stylar and stylar canal areas indicated the presence of heteromorphism with area increasing from the S to M to L morph in both cases. To our knowledge the only previous work on stylar canal differences among floral morphs in a heterostylous taxa is by Dowrick (1956) in *Primula obconica.* Dowrick (1956) noted that the area of conducting tissue of the L morph was only half that of the S morph and that area in both cases increased from diploids to tetraploids. The former pattern is the opposite to that observed in *P. sagittata* (Table 3).

Calculations of the number of pollen tubes that can occupy the stylar canal in *P. sagittata,* based on the presence of polymorphisms in both pollen tube width (see Scribailo and Barrett, 1991) and stylar canal area among the morphs (Table 3), indicate that different packing constraints on the number of pollen tubes present in the style can occur in the floral morphs. The possibility of similar differences between the floral morphs in other heterostylous taxa warrants further investigation since differences in area of stylar canals could have important implications for pollen tube growth and seed set levels, particularly in multiovulate species (e.g., see Barrett, 1980).

Observations of changes in cross-sectional area of the stylar canal at different levels indicates that by the midpoint of the style the trilobed canal narrows and separates into two

sterile canals and a fertile canal of reduced area (except in some styles of the S morph). Studies of pollen tube growth in all pollination types indicate a marked attrition in pollen tube numbers that coincided with the location of this structural bottleneck in the stylar canal. In addition, observations of the apparent preferential growth of pollen tubes into fertile stylar canals is suggestive of a mechanism of pollen tube guidance in the species (Scribailo and Barrett, 1991). These features of the pollen tube pathway in *P. sagittata* are likely to have important reproductive consequences through their effects on pollen tube growth.

Size dimorphisms in stigmatic papillae have been reported in the majority of distylous taxa that have been examined (Ganders, 1979; Gibbs, 1986; Dulberger, 1987). Stigmatic papillae of the L morph are almost always significantly larger than those of the S morph. In addition to the basic size dimorphism of stigmatic papillae in distylous taxa, structural and cytochemical differences in the stigmas of the morphs have also been reported in *Primula obconica* and several *Linum* species. In *Primula obconica* the papillae of the L morph are of the wet type, with a cuticle that accumulates lipidic globules beneath the surface and eventually ruptures, forming a blistery exudate. The S morph has a dry stigma that accumulates small lipidic droplets beneath the cuticle surface of the stigmatic papillae, although the cuticle never ruptures during the secretory process (Schou, 1984; Schou and Mattsson, 1985). In *Linum grandiflorum* a similar situation occurs, but the stigmatic properties of the morphs are reversed (Dulberger, 1974, 1975a, 1987; Ghosh and Shivanna, 1980a, b, 1982). In *Forsythia* both morphs have wet stigmas (Dumas, 1974).

Although the floral morphs in *P. sagittata* vary in the degree of wetness of the stigma and in stigmatic papillae length, we failed to detect differences in the basic cytochemical properties of stigmatic papillae among the floral morphs. Nevertheless, observations of pollen germination after legitimate and illegitimate pollination do suggest that varying degrees of wetness of the stigma surface may be of importance in promoting legitimate matings (Scribailo and Barrett, 1991). The presence of wet stigmas in *P. sagittata* and a number of distylous taxa (see Gibbs, 1986) is at variance with the often cited correlation of dry stigmas usually being associated with sporophytic self-incompatibility (Knox, 1984).

The cytochemical and structural properties of the stigma surface of *P. sagittata* bear a close resemblance to stigmas found in an array of monocotyledonous families, all of which possess gametophytic self-incompatibility. Cytochemically, stigmas of *P. sagittata,* as well as those of *Eichhornia crassipes* (Kandasamy and Vivekanandan, 1983), fall into the monocotyledonous class of stigmas with hydrophilic secretions containing proteins, carbohydrates, and usually lipids (Knox, 1984).

Stigmas of a number of families of monocotyledons are difficult to categorize as wet or dry using the classification system of Heslop-Harrison and Heslop-Harrison (1982). The system primarily classifies stigmas as wet or dry depending on whether the cuticle of the stigmatic papillae ruptures during the secretory process. Cytochemically, the two types of stigmas are usually distinguished by the continuity of the pellicle after nonspecific esterase staining (Shivanna, Heslop-Harrison, and Heslop-Harrison, 1978; Shivanna and Sastri, 1981). In dry stigmas the pellicle forms a continuous layer over the papillae surface. In contrast, blistering of the cuticle in wet stigmas causes the pellicle to fragment and release accumulated substances that then become part of the overall exudate.

Much of the difficulty with the classification of monocotyledonous stigmas stems from the nature of the pollen tube pathway, with the stylar canal often opening directly onto the stigma surface, as it does in the Commelinaceae (Owens et al., 1984). Consequently, the stigma is often secondarily inundated by exudate produced by the stylar canal cells. The problem, therefore, involves determining whether the stigmatic papillae are secretory, and if so, the relative contributions of stigmatic papillae vs. stylar canal cells to the wetness of the stigma (Heslop-Harrison, 1981).

In *P. sagittata,* observations of stigma cytochemistry and nonspecific esterase activity in particular indicate that the cuticle does not rupture during anthesis. The structure of the stigmatic papillae is similar to that which has been reported for *Crocus* (Heslop-Harrison, 1977) and *Gladiolus* (Iridaceae) (Clarke et al., 1977) and members of the Commelinaceae (Stevenson and Owens, 1978; Owens et al., 1984). In these taxa the stigma is of the dry type, because the cuticular layer that is continuous from the stigmatic papillae to the ovary, never ruptures. However, the stigma of *P. sagittata* differs in being classified as wet, because although the cuticle does not rupture, the stigma is apparently secondarily inundated by stylar canal exudates. A similar situation occurs in *Lilium* (Rosen, 1972) and in *Crinum* and *Amaryllis* (Amaryllidaceae) (Shivanna and Sastri, 1981).

The unruptured pellicle and cuticle of the stigmatic papillae in *P. sagittata* indicate that if secretion occurs it must move across the cuticle. Dry stigmas with this type of secretion process seldom exhibit exudate accumulation of the level observed here (particularly in the L morph) (Knox, 1984). Therefore, it seems plausible to suggest that the majority of exudate present on the stigma surface in *P. sagittata* may originate from the stylar canal, although further study would be required to definitively determine the origin of exudate on the stigma surface.

The most striking feature of the ovule in *P. sagittata* is the presence of an integumentary obturator, a structure which, to the best of our knowledge, has not been previously reported in the Pontederiaceae. Obturators are usually defined as any structure that appears to be associated with directing pollen tubes toward the micropyle (Davis, 1966). They are most commonly found in the Euphorbiaceae, Rosaceae, and Liliaceae and are of placental and funicular origin in the majority of species examined (Sterling, 1964; Tilton and Horner, 1980). Integumentary obturators of the type found in *P. sagittata* appear to be quite rare.

Obturators may physically direct the growth of pollen tubes by progressively narrowing the path down which pollen tubes can grow until they enter the micropyle (Steffen, 1951; Heslop-Harrison and Heslop-Harrison, 1986). It has also been postulated that the obturator may act chemotropically, secreting signals that approaching pollen tubes can use as directional cues (Tilton et al., 1984; Arbeloa and Herrero, 1987; Herrero and Arbeloa, 1989), although a chemotropic factor has never been isolated (Heslop-Harrison and Heslop-Harrison, 1986; Heslop-Harrison, 1987).

In contrast to the more typical situation where obturators are small localized pads or swellings near the micropyle of the ovule (Tilton et al., 1984), the degree of elaboration of cells of the obturator in *P. sagittata* is extensive. Although this elaboration suggests a functional role for the obturator, possibly in pollen tube guidance, cells of this structure (Fig. 43) do not have the anatomy of typical secretory cells (Fig. 36). Furthermore, no evidence of exudate was observed on the surface of the papillae of the obturator (Figs. 43–47). It also appears unlikely that the obturator acts as a physical guide since it is spatially separated from the point at which the pollen tubes enter the ovary from the stylar canal (Fig. 42, large arrow). Nevertheless, observations from studies of pollen tube growth in *P. sagittata* indicate differential recognition of the obturator by legitimate and illegitimate pollen tubes. In the latter case pollen tubes either fail to penetrate the obturator and effect fertilization or continue growth past the obturator (Scribailo and Barrett, 1991).

This study has described heteromorphic floral characters in *P. sagittata* and discussed their possible influence on the process of pollination, pollen germination, and pollen tube growth. In addition, we have drawn attention to several similarities between the structural features of the pollen tube pathway in *P. sagittata* and monocotyledonous taxa with gametophytic self-incompatibility. In common with these taxa the ancestors of tristylous members of the Pontederiaceae most likely possessed wet stigmas, hollow styles, and a trimerous floral organization. The possession of these features is likely to have strongly influenced the expression of tristyly as it developed within the Pontederiaceae. The discovery of ovarian sites of cessation of incompatible pollen tube growth in *Pontederia* (Anderson and Barrett, 1986; Scribailo and Barrett, 1991) is a characteristic shared with a number of monocotyledonous taxa with gametophytic self-incompatibility (Stout and Chandler, 1933; Sears, 1937; Brock, 1954; Brewbaker and Gorrez, 1967; Brandham and Owens, 1978; Seavey and Bawa, 1986). The presence of ovarian sites of cessation for pollen tube growth in *Pontederia* are in contrast to the stigmatic and stylar sites found in most species with heteromorphic incompatibility (e.g., see Bawa and Beach, 1983; Richards, 1986). This difference suggests an important influence of structural features of the pollen tube pathway on incompatibility behavior in *Pontederia,* one likely reflecting the monocotyledenous ancestry of the genus.

## LITERATURE CITED

ANDERSON, J. M., AND S. C. H. BARRETT. 1986. Pollen tube growth in tristylous *Pontederia cordata* (Pontederiaceae). *Canadian Journal of Botany* 64: 2602–2607.

ARBELOA, A., AND M. HERRERO. 1987. The significance of the obturator in the control of pollen tube entry into the ovary in peach (*Prunus persica*). *Annals of Botany* 60: 681–685.

BARRETT, S. C. H. 1977. The breeding system of *Pontederia rotundifola* L., a tristylous species. *New Phytologist* 78: 209–220.

———. 1980. Dimorphic incompatibility and gender in *Nymphoides indica* (Menyanthaceae). *Canadian Journal of Botany* 58: 1938–1942.

———. 1990. The evolution and adaptive significance of heterostyly. *Trends in Ecology and Evolution* 5: 144–148.

BAWA, K. S., AND J. H. BEACH. 1983. Self-incompatibility systems in the Rubiaceae of a tropical lowland forest. *American Journal of Botany* 70: 1281–1288.

BENES, K. 1968. On the stainability of plant cell walls with alcian blue. *Biologia Plantarum* 10: 334–347.

BRANDHAM, P. E., AND S. J. OWENS. 1978. The genetic control of self-incompatibility in the genus *Gasteria* (Liliaceae). *Heredity* 40: 165–169.

BREWBAKER, J. L., AND D. D. GORREZ. 1967. Genetics of self-incompatibility in the monocot genera, *Ananas* (pineapple) and *Gasteria*. *American Journal of Botany* 54: 611–616.

BROCK, R. D. 1954. Fertility in *Lilium* hybrids. *Heredity* 8: 409–420.

CLARKE, A. E., J. A. CONSIDINE, R. WARD, AND R. B. KNOX. 1977. Mechanism of pollination in *Gladiolus*: role of the stigma and pollen tube guide. *Annals of Botany* 41: 15–20.

CRUDEN, R. W., AND D. L. LYONS. 1985. Correlations among stigma depth, style length, and pollen grain size: do they reflect function or phylogeny? *Botanical Gazette* 146: 143–149.

DARWIN, C. 1877. The different forms of flowers on plants of the same species. John Murray, London.

DAVIS, G. L. 1966. Systematic embryology of the angiosperms. John Wiley and Sons, New York.

DOWRICK, V. P. J. 1956. Heterostyly and homostyly in *Primula obconica*. *Heredity* 10: 219–236.

DULBERGER, R. 1970. Tristyly in *Lythrum junceum*. *New Phytologist* 69: 751–759.

———. 1974. Structural dimorphism of stigmatic papillae in distylous *Linum* species. *American Journal of Botany* 61: 238–243.

———. 1975a. Intermorph structural differences between stigmatic papillae and pollen grains in relation to incompatibility in Plumbaginaceae. *Proceedings of the Royal Society of London, Series B*, 188: 257–274.

———. 1975b. S-gene action and the significance of characters in the heterostylous syndrome. *Heredity* 35: 407–415.

———. 1981. Dimorphic exine sculpturing in three distylous species of *Linum* (Linaceae). *Plant Systematics and Evolution* 139: 113–119.

———. 1987. Fine structure and cytochemistry of the stigma surface and incompatibility in some distylous *Linum* species. *Annals of Botany* 59: 203–217.

———. 1989. The apertural wall in pollen of *Linum grandiflorum*. *Annals of Botany* 63: 421–431.

DUMAS, C. 1974. Some aspects of stigmatic secretion of *Forsythia*. *In* H. F. Linskens [ed.], Fertilization in higher plants, 119–126. North-Holland, Amsterdam.

ECKENWALDER, J. E., AND S. C. H. BARRETT. 1986. Phylogenetic systematics of the Pontederiaceae. *Systematic Botany* 11: 373–391.

ESSER, K. 1953. Genomverdopplung und Pollensch-Lauchwachstum bei Heterostylen. *Zeitschrift fur induktive Abstammungs- und Vererbungslehre* 85: 28–50.

FEDER, N., AND T. P. O'BRIEN. 1968. Plant microtechnique: some principles and new methods. *American Journal of Botany* 55: 123–142.

FULCHER, R. G., AND S. I. WONG. 1980. Inside cereals—a fluorescence microchemical view. *In* G. E. Inglett and L. Munck [eds.], Cereals for food and beverages, 1–26. Academic Press, New York.

GANDERS, F. R. 1979. The biology of heterostyly. *New Zealand Journal of Botany* 17: 607–635.

GHOSH, S., AND K. R. SHIVANNA. 1980a. Pollen-pistil interaction in *Linum grandiflorum*: scanning electron microscopic observations and proteins of the stigma. *Planta* 149: 257–261.

———, AND ———. 1980b. Pollen-pistil interactions in *Linum grandiflorum*; stigma surface proteins and stigma receptivity. *Indian National Academy of Science* 46: 177–183.

———, AND ———. 1982. Studies on pollen-pistil interaction in *Linum grandiflorum*. *Phytomorphology* 32: 385–395.

GIBBS, P. E. 1986. Do homomorphic and heteromorphic self-incompatibility systems have the same sporophytic mechanism? *Plant Systematics and Evolution* 154: 285–323.

GLOVER, D. E., AND S. C. H. BARRETT. 1983. Trimorphic incompatibility in Mexican populations of *Pontederia sagittata* Presl (Pontederiaceae). *New Phytologist* 95: 439–455.

HERRERO, M., AND A. ARBELOA. 1989. Influence of the pistil on pollen tube kinetics in peach (*Prunus persica*). *American Journal of Botany* 76: 1441–1447.

HESLOP-HARRISON, J. 1979. Aspects of the structure, cytochemistry and germination of the pollen of rye (*Secale cereale* L.). *Annals of Botany* 1: 1–47 (Supplement).

———. 1987. Pollen germination and pollen tube growth. *In* K. L. Giles and J. Prakash [eds.], International review of cytology, vol. 107, 59–73. Academic Press, Toronto.

———, AND Y. HESLOP-HARRISON. 1982. The specialized cuticles of the receptive surfaces on angiosperm stigmas. *In* D. F. Cutler, K. L. Alvin, and C. E. Price [eds.], The plant cuticle, 99–120. Academic Press, Toronto.

———, AND ———. 1986. Pollen-tube chemotropism: fact or delusion? *In* M. Cresti and R. Dallai [eds.], Biology of reproduction and cell motility in plants and animals, 169–174. University of Sienna, Sienna.

———, AND K. R. SHIVANNA. 1977. The receptive surface of the angiosperm stigma. *Annals of Botany* 41:1233–1258.

HESLOP-HARRISON, Y. 1977. The pollen-stigma interaction: pollen tube penetration in *Crocus*. *Annals of Botany* 41: 913–922.

———. 1981. Stigma characteristics and angiosperm taxonomy. *Nordic Journal of Botany* 1: 401–420.

HOLLANDER, M., AND D. A. WOLFE. 1973. Nonparametric statistical methods. John Wiley and Sons, New York.

JENSEN, W. A. 1962. Botanical histochemistry. W. H. Freeman, San Francisco.

KANDASAMY, M. K., AND M. VIVEKANANDAN. 1983. Biochemical composition of stigmatic exudate of *Eichhornia crassipes* (Mart.) Solms. *Aquatic Botany* 16: 41–47.

KNOX, R. B. 1984. Pollen-pistil interactions. *In* H. F. Linskens and J. Heslop-Harrison [eds.], Cellular interactions. Encyclopedia of plant physiology, new series vol. 17, 508–608. Springer-Verlag, New York.

LEWIS, D. 1942. Physiology of incompatibility in plants. I. The effect of temperature. *Proceedings of the Royal Society of London, Series B* 131: 13–26.

———. 1943. Physiology of incompatibility in plants. II. *Linum grandiflorum*. *Annals of Botany* 2: 115–122.

LLOYD, D. G., AND C. J. WEBB. In press a. Evolution of heterostyly. *In* S. C. H. Barrett [ed.], Evolution and function of heterostyly. Springer-Verlag, Berlin.

———, AND ———. In press b. Selection of heterostyly. *In* S. C. H. Barrett [ed.], Evolution and function of heterostyly. Springer-Verlag, Berlin.

———, ———, AND R. DULBERGER. 1990. Heterostyly in species of *Narcissus* (Amaryllidaceae), *Hugonia*

(Linaceae) and other disputed cases. *Plant Systematics and Evolution* 172: 215–227.

LUFT, J. H. 1961. Improvements in epoxy resin embedding methods. *Journal of Biophysical and Biochemical Cytology* 9: 409–414.

MATHER, K., AND D. DEWINTON. 1941. Adaptation and counter-adaptation of the breeding system in *Primula*. *Annals of Botany* 5: 297–311.

MULCAHY, D. 1965. Heterostyly within *Nivenia* (Iridaceae). *Brittonia* 17: 349–351.

ORNDUFF, R. 1966. The breeding system of *Pontederia cordata* L. *Bulletin of the Torrey Botanical Club* 93: 407–416.

OWENS, S. J., S. MCGRATH, M. A. FRASER, AND L. R. FOX. 1984. The anatomy, histochemistry and ultrastructure of stigmas and styles in Commelinaceae. *Annals of Botany* 54: 591–603.

PEARSE, A. G. E. 1972. Histochemistry: theoretical and applied, vol. 1. Churchill-Livingston, London.

PLITMAN U., AND D. A. LEVIN. 1983. Pollen-pistil relationships in the Polemoniaceae. *Evolution* 37: 957–967.

POPPER, H. 1944. Distribution of vitamin A in tissue as visualized by fluorescence microscopy. *Physical Review* 24: 204–224.

PRICE, S. D., AND S. C. H. BARRETT. 1982. Tristyly in *Pontederia cordata* L. (Pontederiaceae). *Canadian Journal of Botany* 60: 897–905.

RICHARDS, A. F. 1986. Plant breeding systems. George, Allen and Unwin, Boston.

RICHARDS, J. H., AND S. C. H. BARRETT. 1984. The developmental basis of tristyly in *Eichhornia paniculata* (Pontederiaceae). *American Journal of Botany* 71: 1347–1363.

———, AND ———. 1987. Development of tristyly in *Pontederia cordata* (Pontederiaceae). I. Mature floral structure and patterns of relative growth of reproductive organs. *American Journal of Botany* 74: 1831–1841.

ROSEN, W. G. 1972. Pistil pollen interactions in *Lilium*. *In* J. Heslop-Harrison [ed.], Pollen development and physiology, 239–254. Butterworths, London.

SAS. 1987. Statistical analysis system. User's guide: statistics, version 6. SAS Institute, Cary, NC.

SCHOU, O. 1984. The dry and wet stigmas of *Primula obconica*: ultrastructural and cytochemical dimorphisms. *Protoplasma* 121: 99–113.

———, AND O. MATTSSON. 1985. Differential localization of enzymes in the stigmatic exudates of *Primula obconica*. *Protoplasma* 125: 65–74.

SCRIBAILO, R. W., AND S. C. H. BARRETT. 1991. Pollen-pistil interactions in tristylous *Pontederia sagittata* (Pontederiaceae). II. Patterns of pollen tube growth. *American Journal of Botany* 78: 1662–1682.

SEARS, E. R. 1937. Cytological phenomena connected with self-sterility in flowering plants. *Genetics* 22: 130–181.

SEAVEY, S. R., AND K. S. BAWA. 1986. Late-acting self-incompatibility in angiosperms. *Botanical Review* 51: 195–219.

SHIVANNA, K. R., J. HESLOP-HARRISON, AND Y. HESLOP-HARRISON. 1981. Heterostyly in *Primula* 2. Sites of pollen inhibition, and effects of pistil constituents on compatible and incompatible pollen-tube growth. *Protoplasma* 107: 319–337.

———, ———, AND ———. 1983. Heterostyly in *Primula* 3. Pollen water economy: a factor in the intramorph-incompatibility response. *Protoplasma* 117: 175–184.

———, Y. HESLOP-HARRISON, AND J. HESLOP-HARRISON. 1978. The pollen-stigma interaction: bud pollination in the Cruciferae. *Acta Botanica Neerlandica* 27: 107–119.

———, AND D. C. SASTRI. 1981. Stigma-surface esterase activity and stigma receptivity in some taxa characterized by wet stigmas *Annals of Botany* 47: 53–64.

SMITH, W. R. 1898. A contribution to the life history of the Pontederiaceae. *Botanical Gazette* 25: 324–337.

SOKAL, R. R., AND F. J. ROHLF. 1981. Biometry. W. H. Freeman, San Francisco.

STEFFEN, K. 1951. Zur Kenntnis des Befruchtungsvorganges bei *Impatiens glandulifera* Lindl. Cytologische studien am Embryosack der Balsamineen. *Planta* 39: 175–244.

STERLING, C. 1964. Comparative morphology of the carpel in the Rosaceae. I. Prunoideae: *Prunus*. *American Journal of Botany* 51: 36–44.

STEVENS, V. A. M., AND B. G. MURRAY. 1982. Studies on heteromorphic self-incompatibility systems: physiological aspects of the incompatibility system of *Primula obconica*. *Theoretical and Applied Genetics* 61: 245–256.

STEVENSON, D. W., AND S. J. OWENS. 1978. Some aspects of the reproductive morphology of *Gibasis venustula* (Kunth) D. R. Hunt (Commelinaceae). *Botanical Journal of the Linnean Society* 77: 157–175.

STOUT, A. B., AND C. CHANDLER. 1933. Pollen-tube behavior in *Hemerocallis* with special reference to incompatibilities. *Bulletin of the Torrey Botanical Club* 60: 397–417.

TILTON, V. R., AND H. T. HORNER. 1980. Stigma, style, and obturator of *Ornithogalum caudatum* (Liliaceae) and their function in the reproductive process. *American Journal of Botany* 67: 1113–1131.

———, L. W. WILCOX, R. G. PALMER, AND M. C. ALBERTSEN. 1984. Stigma, style, and obturator of soybean, *Glycine max* (L.) Merr. (Leguminosae) and their function in the reproductive process. *American Journal of Botany* 71: 676–686.